Transient moisture profiles in cover-zone concrete during water absorption

SHORT COMMUNICATION

Transient moisture profiles in cover-zone concrete during water absorption

W. J. McCarter *

G. Alaswad

B. Suryanto

School of Energy, Geoscience, Infrastructure and Society,

Heriot Watt University,

Edinburgh, EH14 4AS,

UK

* Corresponding Author: E-mail: w.j.mccarter@hw.ac.uk

Tel: +44 (0)131 451 3318

ORCID

William J McCarter: 0000-0002-1949-2856

Benny Suryanto: 0000-0002-3979-9994

Abstract

A number of sophisticated techniques, such as NMR imaging and γ-ray attenuation, have now been used to study moisture transport in porous construction materials. This paper presents initial developments in the application of discretized, electrical conductivity measurements as a relatively simple technique to monitor water movement within cover-zone concrete. Using a 3-phase model and the Archie relationship for porous rock formations, conductivity measurements are used to evaluate moisture-content profiles during water ingress and, through the use of Boltzmann's transformation, it is shown that these profiles *collapse* onto a *master-curve*. Having obtained the master-curve during absorption, the capillary transport coefficient (D_0) can then be obtained; however, the current work focuses on presenting the methodology as an alternative testing technique.

Keywords: concrete, water-absorption, monitoring, conductivity, moisture profiles, Boltzmann transform

1. Introduction

The penetration of water into porous construction materials, as well deleterious ions dissolved in it (e.g. chlorides, sulphates), is of considerable importance as virtually all deterioration processes are as a direct result of water ingress. It is thus highly desirable to be able to predict, for a given set of conditions (e.g. environmental exposure, concrete mix), the depth and rate of water penetration and solute concentration profile as they develop over time as this, ultimately, allows estimation of the rate of degradation of the structure and residual service life.

The capillary transport (or moisture diffusion) coefficient (D_θ) is a fundamental moisture transfer parameter and its determination is essential in the simulation of moisture movement. D_θ can be evaluated from the transient moisture profiles obtained during water absorption. Monitoring the time-variant water-content profiles has been undertaken on a range of porous materials such as fired-clay brick, limestone, plaster, cement pastes, mortars and concretes using nuclear magnetic resonance (NMR) imaging [see, for example, 1-7], other techniques include γ-ray attenuation [8], X-ray radiography [9, 10] and neutron radiography and tomography [11]. When investigating cementitious materials using NMR, complications can occur if the binder contains paramagnetic oxides (e.g. Fe, Mn) hence much work tends to be undertaken using white cement. A more simple gravimetric technique, using a standard water-absorption test, has also been developed to obtain moisture profiles in a clayey aerated concrete [12]; however, this method involves cutting specimens so is destructive in nature.

In this paper we present initial studies on the application of discretized, in-situ, electrical conductivity measurements within the surface region of concrete samples to evaluate the transient moisture profiles during water absorption.

2. Background Theory and Current Developments

The flow of water into a porous surface – concrete in this instance – with a uniform initial water-content is described by Fick's 2nd Law for 1-D, non-linear diffusion,

$$\frac{\partial \Theta}{\partial t} = \frac{\partial}{\partial x}\left(D_{\Theta} \frac{\partial \Theta}{\partial x} \right) \tag{1}$$

where, in this instance, Θ is the reduced or normalised water content, D_{Θ} is the capillary transport coefficient (diffusivity), t is time and *x* is the spatial distance from the inflow surface where water is applied. The normalised water-content, Θ_t, at time, t, is further defined as,

$$\Theta_t = \left(\frac{\theta_t - \theta_i}{\theta_s - \theta_i} \right) \tag{2}$$

where θ_i is the initial water-content of the material, θ_s is the saturated water-content and θ_t is the water-content at time, t, after the start of absorption. The water-content is expressed on a volumetric basis. Equation (1) can be transformed into an ordinary differential equation by introducing the Boltzmann transformation $\lambda = xt^{-1/2}$ with the boundary conditions $\lambda = \infty$ (Θ = 0 at time, t = 0)), and $\lambda = 0$ ($\Theta = 1$ as $t \rightarrow \infty$)). Hence, during water absorption, all moisture profiles are related by a similar $t^{1/2}$ scaling and by plotting the transient moisture profiles, $\Theta(x, t)$, against λ produces a master profile which is time invariant. Having obtained the master curve from the experimental data, the capillary transport coefficient, D_{Θ}, can then be calculated from a derivative and an area of the Boltzmann's curve as follows,

$$D_{\Theta} = -\frac{1}{2}\frac{1}{\left(\frac{d\Theta}{d\lambda}\right)_{\Theta_t}} \int_{\Theta_i}^{\Theta_t} \lambda \, d\Theta \quad = -\frac{1}{2}\frac{1}{S_{\Theta_t}} \, \Omega_{(\Theta_i - \Theta_t)} \tag{3}$$

which is shown schematically on Fig. 1 where $\Omega_{(\Theta i - \Theta t)}$ is the area bounded by the curve $\Theta(\lambda)$ between Θ_i and Θ_t and $S_{\Theta t}$ is the slope of the $\Theta(\lambda)$ curve at a normalized water-content of Θ_t.

In the current study, we have replaced the volumetric water content in equation (2) by the electrical conductivity of the concrete obtained from in-situ measurements. With reference to Fig. 2, unsaturated concrete has been simplified as a three phase system comprising solids (aggregate, unhydrated binder and products of hydration), capillary pore-water and air-filled capillary pores. The porosity of the concrete is denoted, ϕ, and the degree of capillary pore saturation is S_r. If the solids (and air) can be assumed to be non-conductive, then the conductivity of the concrete will be directly related to the volume fraction of pore-water and its conductivity, denoted σ_p. If a unit cube of material (unit length into the plane of the page) is placed between a pair of electrodes, the conductivity of the concrete, σ_c, will be,

$$\sigma_c = \frac{L}{R_p A} \tag{4}$$

where, for a prismatic sample, L is the distance between the electrodes (= 1.0), A is the cross-sectional area of the electrodes (= 1.0×1.0) and R_p is the resistance of the pore-fluid. The resistance, R_p, of the pore fluid is also given by,

$$R_p = \frac{L}{\sigma_p A'} \tag{5}$$

Where L = 1.0 as above, and A' is the cross-sectional area available for conduction through the pore-fluid. From Fig. 1, A' = $S_r\phi \times 1.0$ as unit cube is assumed, hence, as a first approximation, the conductivity of the concrete could be written as,

$$\sigma_c = \sigma_p S_r \phi \tag{6}$$

$S_r\phi$ is the volumetric water-content, θ, defined above; however, this assumes a *straight-tube* capillary model and does not take account of the tortuosity, connectedness and constricted nature of the capillary pore network. Adapting Archie's law [13] which was developed for porous rock formations, the cross-sectional area available for conduction will be reduced from $S_r\phi$ to $(S_r\phi)^m$ where the exponent *m* is in the range 1.5-3.0 for rocks. With regards to cementitious materials, values of *m* in the range ~3.0-5.0 have been reported [14, 15], hence,

$$S_r\phi = \theta \approx \left(\frac{\sigma_c}{\sigma_p}\right)^{\frac{1}{m}} \tag{7}$$

If it is tacitly assumed that the pore-water conductivity remains constant, then equation (2) can be written in terms of conductivity,

$$\Theta(t) \approx \left(\frac{\left(\frac{\sigma_{c,t}}{\sigma_{c,i}}\right)^{1/m} - 1}{\left(\frac{\sigma_{c,s}}{\sigma_{c,i}}\right)^{1/m} - 1}\right) \tag{8}$$

Where $\sigma_{c,i}$ is the conductivity of the concrete prior to the start of the absorption test, $\sigma_{c,s}$ is the conductivity of the saturated concrete and $\sigma_{c,t}$ is the conductivity of the concrete at time, t, after the start of the absorption test. A value of $m = 4.0$ [15] has been adopted in the current work

3. Experimental Programme

In order to monitor both the temporal and spatial changes of moisture movement in concrete a test-cell was designed such that electrical measurements (resistance in this instance) could be made at discrete depths from the exposed surface of the concrete samples.

3.1 Materials

In the work presented, the binders comprised ordinary Portland cement clinker, CEM I 52.5N to EN197-1 [16] and CEM I cement blended with a low-lime fly-ash to EN450-1 [17]. The concrete mixes used in the current study are presented in Table 1, together with their respective 28-day (f_{28}) and 180-day (f_{180}) compressive strengths after continuous submerged curing at 21°C±1°C. A crushed rock (granite) coarse aggregate and matching crushed rock fines were used throughout (100% passing the 5mm sieve, 8% passing the 150μm sieve). The aggregate was conditioned to a saturated surface dry state. The aggregate content was adjusted to ensure that the mass of binder remained constant for each water-binder (w/b) ratio. The following were cast for each mix: six samples placed in cylindrical test-cells (detailed below) and three, 100mm cubes for the compressive strength tests.

3.2 Test Cells

Concrete samples were cast in 182mm (outside diameter) and 200mm (high) PVC moulds. One end of the cylinder was attached to 12mm plywood base-plate and the concrete surface cast against the plywood was used as the working surface; the plywood had been given a coat of proprietary release-agent prior to casting. Pairs of stainless steel rod-electrodes, were inserted through the side of the mould shown schematically in Fig. 3. The rod-electrodes were 2.4mm in diameter and sleeved to expose a 20mm tip. Within each electrode pair, electrodes were positioned at 12mm centre to centre (c/c) and protruded 50mm into the sample. With reference to Fig. 3, five electrode-pairs were positioned at 10mm intervals at depths from 10 to 50mm from the working surface with a 30° offset; a pair of electrodes was also positioned at 100mm and at 175mm from the working surface. The electrode-pairs within the test-cell were calibrated by filling the cell with solutions of known conductivity thereby allowing the concrete resistance, R_c (ohms), measured across the electrodes to be

converted to conductivity, σ_c (S/cm), by,

$$\sigma_c = \frac{k}{R_c} \quad (S/cm) \tag{9}$$

where *k* is the (geometrical) calibration constant for the electrode-pair obtained from the calibration procedure. However, as the test-cell had five (geometrically similar) electrode pairs, an average value of *k* was evaluated to give an overall test-cell constant for the electrodes; the value of *k* was obtained as 0.306 cm^{-1} (±5%). It should be noted that a total 5 calibrating solutions were used and covered the anticipated range of concrete conductivity (10^{-3}–10^{-5} S/cm). Two thermistors (for temperature measurements) were cast into the sample and were attached to electrodes positioned at 10mm and 100mm from the exposed surface.

3.3 Ambient Temperature Regime

After casting and compacting, the top (cast) surface of each cell was tightly covered with a plastic sheet so as to prevent evaporation. At 24-hours, the plywood base was removed and the cylinders and the *cast* surface were sealed with two coats of a high-build epoxy paint; also, while the final coat of epoxy was still *tacky*, it was covered with a layer of *cling-film* to add an additional vapour barrier and ensure no moisture movement through this surface. After casting, the samples were placed in an environmental cabinet which was programmed to give a 24-hour temperature cycle of: 10-hours at 40±1°C, 3-hours cooling to 21°C followed by 11-hours at 21±1°C. This was chosen to represent the diurnal temperature fluctuations which can be experienced in hot climates [18, 19]. A relative humidity of 60% was maintained over a saturated sodium bromide solution with the air speed over the samples maintained at approximately 4m/s. The samples remained in the PVC moulds throughout to ensure uniaxial moisture movement and subjected to a 24-hour water absorption test ~75 days after casting. During the absorption test, the samples were maintained at laboratory temperature (21°C).

3.4 Measurements and Data Acquisition

The electrical resistance of the concrete (R_c in ohms) between each pair of electrodes was obtained employing a two-point technique using signal amplitude of 350mV at a frequency of 1kHz. This frequency was optimised from a-priori experiments using impedance spectroscopy to ensure electrode polarization effects were reduced to a minimum [20]. The cabling from the cells was ducted out through a small porthole in the side of the chamber and connected to a resistance meter and multiplexing unit to record the electrical resistance across the electrode-pairs and thermistors. A reading cycle, comprising seven electrode-pair measurements and three thermistor measurements (two embedded within sample and one placed in the environmental cabinet), was initiated every 2 minutes over the 24-hour water absorption cycle.

4. Results and Discussion

For illustrative purposes, Figs. 4(a) and (b) present the change in the conductivity of the concrete during water absorption for PC and FA concrete mixes. Note that for reasons of clarity only every 20th data point is highlighted on each curve. As conductivity values at the different electrode positions can change by more than an order of magnitude during water absorption, this Figure presents the relative change in conductivity, $\sigma_{c,i}/\sigma_{c,t}$, where $\sigma_{c,i}$ and $\sigma_{c,t}$ are, respectively, the measured conductivity just prior to the start of the absorption test and at time, t, after the start of the test. This is the same nomenclature used in Section 2.0 above. As the water-front moves through the surface zone $\sigma_{c,t}$ will increase and the response at a particular electrode-pair is characterised by a well-defined, decreasing portion. The decreasing portion of the curve indicates the arrival of the water-front into the electrical field between that particular electrode-pair; once the water-front has moved beyond the electrical field, a steady-state ratio is achieved and denoted $\sigma_{c,i}/\sigma_{c,s}$, where $\sigma_{c,s}$ is denoted the steady-

state conductivity. It could be assumed that at steady-state, the concrete is in a fully saturated condition in the vicinity of the electrode-pair (see Section 2.0 above). It is evident in these Figures that within the 24-hour absorption test, water had advanced through the surface 0-40mm in ~11 hours for the PC concrete, and 0-50mm in 6 hours for the FA concrete.

Where a steady-state $\sigma_{c,i}/\sigma_{c,s}$ value has been achieved then $\Theta(t)$ versus depth (x) profiles can be evaluated at discrete points in time after the start of the absorption test. From equation (8), $\Theta(t)$ was estimated using the conductivity values measured at each electrode depth (x): from Fig. 4, x = 10, 20, 30 and 40mm for the PC concrete and x = 10, 20, 30, 40 and 50mm for the FA concrete. The resulting normalised moisture profiles at selected times are presented in Figs. 5(a) and (b). By applying the Boltzmann transformation, $\lambda = xt^{-1/2}$, to the moisture profiles in Fig 5, the curves showing $\Theta(t) - \lambda$ dependency for the PC and FA concretes are presented in Figs. 6(a) and (b), respectively. The measurements on each Figure can be combined into a single average master curve for the concrete mix. The master curve can be best represented by a sigmoidal decay curve as follows,

$$\Theta = \left(\frac{1}{1+10^{a[\lambda - b]}} \right) \tag{10}$$

where the fitting parameters a and b for each concrete mix are presented on the respective Figure. Parameter a controls the gradient of the descending portion of the response – as the value of a increases the slope gets more precipitous; b represents the value of λ at which $|d\Theta_t/d\lambda|$ maximises on the decreasing portion of the curve. Equation (10) can be used to evaluate $d\Theta_t/d\lambda$ in equation (3); furthermore, λ can also be derived from equation (10),

$$\lambda = b + \frac{\ln[(1-\Theta)/\Theta]}{a \ln 10} \tag{11}$$

which can then be used to evaluate the integral in equation (3) i.e. $\int_{\Theta_i}^{\Theta_t} \lambda \, d\Theta$.

5. Concluding Comments

The central aim of the work has been to present initial studies utilizing discretized, in-situ electrical conductivity measurements to track the advance of a water-front through the surface zone of concrete and evaluate transient moisture profiles within this region. More specifically, using a simplified electrical model based on the Archie equation, the volumetric water-content of the concrete was approximated in terms of electrical conductivity. It was shown that when these measurements are used in conjunction with the Boltzmann transformation, they can be used to evaluate the master curve for a particular concrete mix. Ultimately, this can provide information on moisture diffusivity which can be used in the simulation of moisture transport processes. In comparison to cost and safety issues associated with other, more sophisticated techniques for evaluating moisture movement, the method represents a much easier approach. Although resolution at this stage may not be as good as, for example, NMR, this can be increased in the proposed method simply by increasing the number of electrode-pairs and the distance between the pairs.

Acknowledgements

One of the Authors (GA) would like to thank Libyan Embassy-Cultural Attaché for their financial support.

Conflict of Interest

The authors declare that they have no conflict of interest.

References

1. R.J. Gummerson, C. Hall, W.D. Hoff, R. Hawkes, G.N. Holland, W.S. Moore, Unsaturated water flow within porous materials observed by NMR imaging, Nature 281(September) (1979) 56-57. DOI: 10.1038/281056a0.
2. A. Leventis, D.A. Verganelakis, M.R. Halse, J.B. Webber, J.H. Strage, Capillary Imbibition and Pore Characterisation in Cement Pastes, Transp. Porous Med., 39(2) (2000) 143-157. DOI: 10.1023/A:1006687114424.
3. K. Hazrati, L. Pel, J Marchand, K. Kopinga, M. Pigeon, Determination of isothermal unsaturated capillary flow in high performance cement mortars by NMR imaging, Mater. Struct. 35(December) (2002) 614-622. DOI 10.1007/BF02480354.
4. D.A. Lockington, J.-Y. Parlange, Anomalous water absorption in porous materials, J. Phys. D: Appl. Phys. 36(6) 2003 760-767. DOI: 10.1088/0022-3727/36/6/320
5. C. Hall, Anomalous diffusion in unsaturated flow: Fact or fiction? Cem. Concr. Res. 37(3) (2007) 378-385. DOI: 10.1016/j.cemconres.2006.10.004.
6. P. Rucker-Gramm, R.E. Beddoe, Effect of moisture content of concrete on water uptake, Cem. Conc. Res. 40(1) (2010) 102-108. DOI: 10.1016/j.cemconres.2009.09.001
7. C. Zhou, General solution of hydraulic diffusivity from sorptivity test, Cem. Concr. Res. 58(April) (2014) 152-160. DOI: 10.1016/j.cemconres.2014.01.019.
8. V. Picandet, G. Bastian, A. Khelidj, Compared imbibitions of ordinary and high performance concrete with null or positive water pressure head, Cem. Concr. Res. 38(6) (2008) 772-782. DOI:10.1016/j.cemconres.2008.01.014.
9. S. Roels, J. Carmeliet, Analysis of moisture flow in porous materials using microfocus X-ray radiography, Int. J. Heat Mass Tran., 49(25), (2006) 4762-4772. DOI: 10.1016/j.ijheatmasstransfer.2006.06.035.

10. V.G. Mossotti, L.M. Castanier, The measurement of water transport in Salem limestone by X-ray computer aided tomography, In: The Engineering Geology of Ancient Works, Monuments and Historical Sites: Preservation and Protection, Proc. of an International Symp. organized by the Greek National Group of IAEG (Eds. P.G. Marinos and G.C. Koukis), Athens, 19–23 September (1988) 2079-82. (Publisher, A.A. Balkema, Rotterdam).
11. D.R.M. Brew, F.C. de Beer, M.J. Radebe, R. Nshimirimana, P.J. McGlinn, L.P. Aldridge, T.E. Payne, Water transport through cement-based barriers - A preliminary study using neutron radiography and tomography, Nucl. Instrum. Meth. A, 605(1) (2009) 163-166. DOI: 10.1016/j.nima.2009.01.146.
12. M.S. Goual, F. de Barquin, M.L. Benmalek, A. Bali, M. Quéneudec, Estimation of the capillary transport coefficient of Clayey Aerated Concrete using a gravimetric technique, Cem. Concr. Res. 30(10) (2000) 1559-1563. DOI: 10.1016/S0008-8846(00)00379-3.
13. G.E. Archie, The electrical resistivity log as an aid in determining some reservoir characteristics, Trans. Am. Inst. of Min. Met. Eng., 146(1) (1942) 54-62. DOI: 10.2118/942054-G
14. M.R. Nokken, R.D. Hooton, Using pore parameters to estimate permeability or conductivity of concrete, Mater. Struct, 41(1) (2008) 1-16. DOI: 10.1617/s11527-006-9212-y.
15. J. Weiss; K. Snyder; J. Bullard, D. Bentz, Using a Saturation Function to Interpret the Electrical Properties of Partially Saturated Concrete, ASCE J. Mater. Civil Eng., 25(8) (2013) 1097-1106. DOI: 10.1061/(ASCE)MT.1943-5533.0000549.
16. British Standards Institution (BSI), BS-EN197-1 Cement-Part 1: Composition, specifications and conformity criteria for common cements, BSI (2011) London UK.

17. British Standards Institution (BSI), BS-EN450-1 Fly ash for concrete. Definition, specifications and conformity criteria, BSI (2012) London, UK.
18. O.S. Baghabra Al-Amoudi, M. Maslehuddin and T.O. Abiola, Effect of type and dosage of silica fume on plastic shrinkage in concrete exposed to hot weather, Constr. Build. Mater., 18(10) (2004) 737-743. DOI: 10.1016/j.conbuildmat.2004.04.031
19. H. Ait-Aider, N.E. Hannachi, and M. Mouret, Importance of W/C ratio on compressive strength of concrete in hot climate conditions, Build. Environ. 42(6) (2007). 2461-2465. DOI: 10.1016/j.buildenv.2006.05.003.
20. W.J. McCarter and R. Brousseau, The A.C. response of hardened cement paste, Cem. Concr. Res. 20(6) (1990) 891-900. DOI: 10.1016/0008-8846(90)90051-X

Captions for Figures

Fig. 1 Schematic diagram showing the normalised water-content as a function of the Boltzmann transform.

Fig. 2 Concrete considered as a simplified three-phase system comprising air, pore-fluid and solids. In this Figure, S_r is the degree of pore saturation and ϕ is the total porosity.

Fig. 3 Test cell showing positioning of electrodes and thermistors (a) sectional view, and (b) plan view.

Fig. 4 Change in conductivity ratio, $\sigma_{c,i}/\sigma_{c,t}$, during the 24-hour absorption cycle for (a) PC concrete and (b) FA concrete.

Fig. 5 Water-content profiles during absorption for (a) PC concrete, and (b) FA concrete (depth *x* is measured from the exposed surface).

Fig. 6 Normalised water-content within a local volume located at various depths from the exposed concrete surface as a function of the Boltzmann transform for (a) PC concrete, and (b) FA concrete.

Table 1 Summary of concrete mixes (w/b = water-binder ratio).

Mix Designation	w/b	CEM I kg/m^3	FA kg/m^3	20mm kg/m^3	10mm kg/m^3	Fine (<5mm) kg/m^3	f_{28} MPa	f_{180} MPa
PC	0.60	290	-	687	458	765	43.4	54.7
FA	0.60	188	102	674	450	748	25.6	40.8

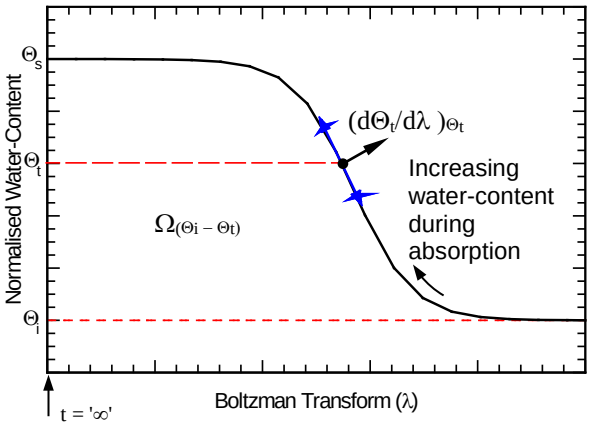
Normalised Water-Content
Θs
Θt
Θi
(dΘt/dλ)Θt
Increasing
water-content
during
absorption
Ω(Θi – Θt)
t = '∞'
Boltzman Transform (λ)

Fig. 1

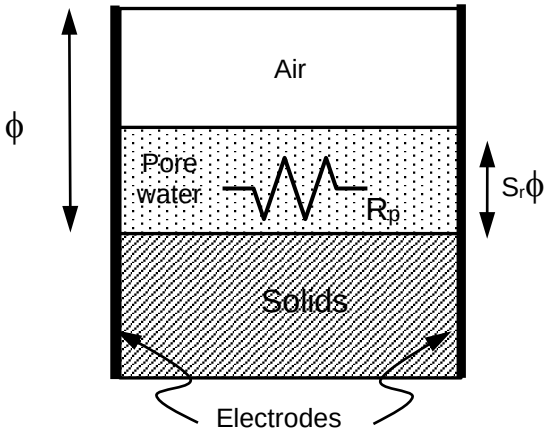

Fig. 2

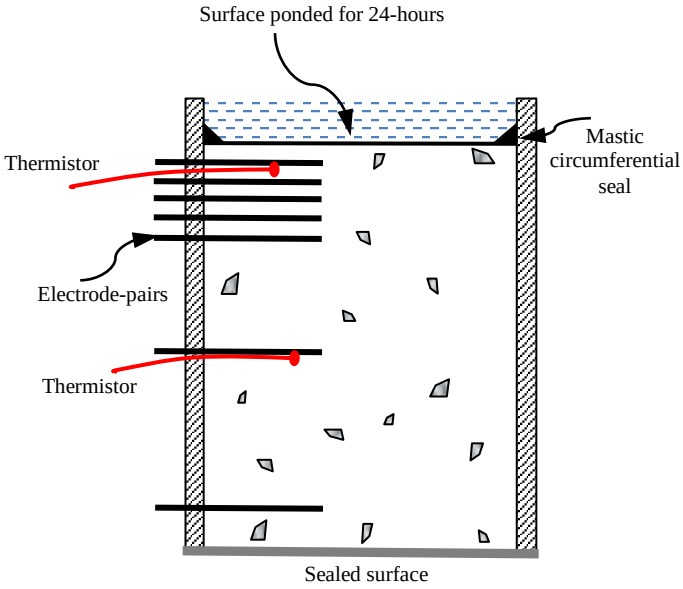
Surface ponded for 24-hours
Thermistor
Mastic
circumferential
seal
Electrode-pairs
Thermistor
Sealed surface

(a)

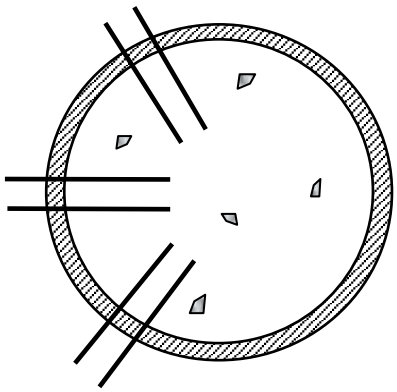

(b)

Fig. 3

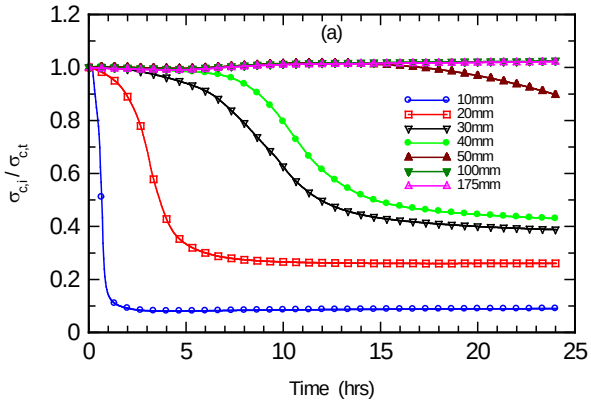
(a)
10mm
20mm
30mm
40mm
50mm
100mm
175mm
$\sigma_{c,i} / \sigma_{c,t}$
Time (hrs)

(a)

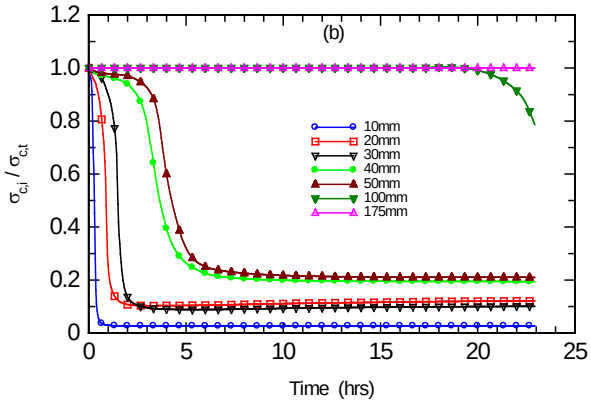
(b)
10mm
20mm
30mm
40mm
50mm
100mm
175mm
$\sigma_{c,i} / \sigma_{c,t}$
Time (hrs)

(b)

Fig. 4

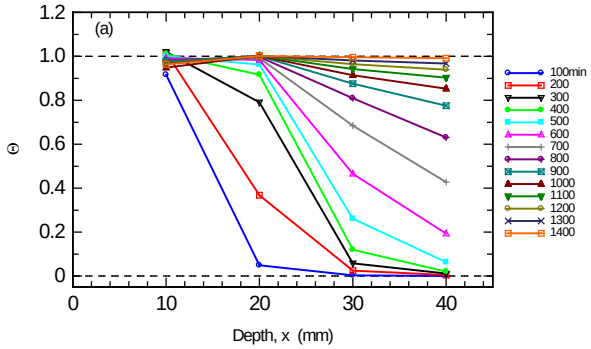
(a)
Θ
Depth, x (mm)
100min
200
300
400
500
600
700
800
900
1000
1100
1200
1300
1400

(a)

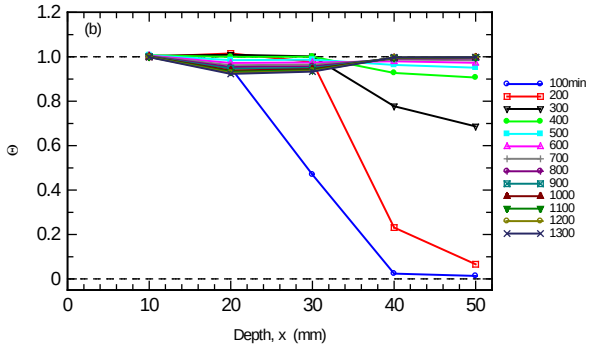
(b)
Θ
Depth, x (mm)
100min
200
300
400
500
600
700
800
900
1000
1100
1200
1300

(b)

Fig. 5

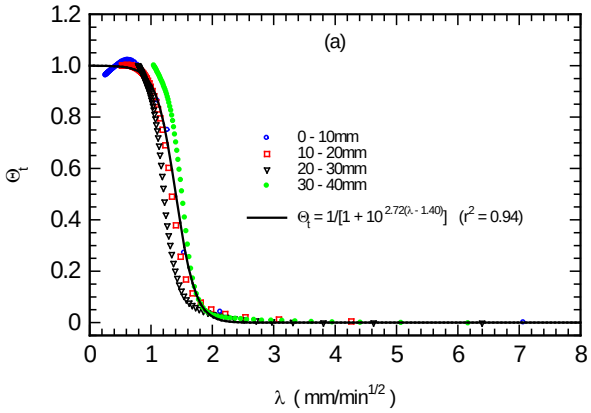
(a)
0 - 10mm
10 - 20mm
20 - 30mm
30 - 40mm
Θt = 1/[1 + 10^2.72(λ - 1.40)] (r^2 = 0.94)
Θt
λ (mm/min^1/2)

(a)

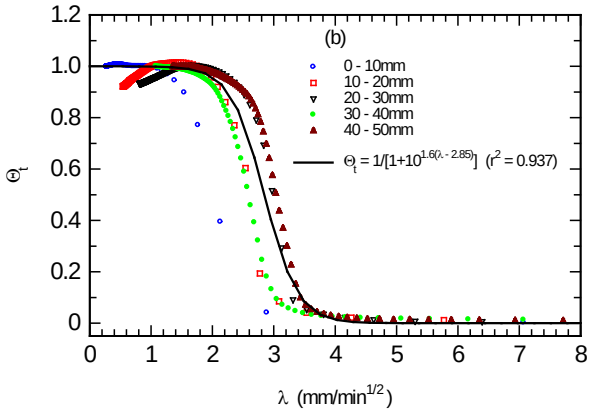
(b)
0 - 10mm
10 - 20mm
20 - 30mm
30 - 40mm
40 - 50mm
Θt = 1/[1+10^1.6(λ - 2.85)] (r^2 = 0.937)
Θt
λ (mm/min^1/2)

(b)

Fig. 6